RSC Advances

ROYAL SOCIETY OF CHEMISTRY

www.rsc.org/advances

Temperature-responsive hydroxypropylcellulose based thermochromic material and its smart window application

Yong-Sheng Yang, Yang Zhou, Freddy Boey Yin Chiang* and Yi Long*

School of Materials Science and Engineering, Nanyang Technological University, 50 Nanyang Avenue, Singapore 639798

Corresponding author, Prof. Freddy Boey Yin Chiang: mycboey@ntu.edu.sg, Dr. Yi Long: longyi@ntu.edu.sg

Abstract: Thermochromic materials are the most cost effective smart window materials and the organic hydrogel material has large solar modulating ability (ΔT_{sol}) and the luminous transmittance (T_{lum}) compared with inorganic VO_2 based materials. Here we report a green and new organic thermochroic material based on hydroxypropylcellulose. With increasing addition of NaCl from 0.5% (wt. %) to 5% (wt. %), the LCST (lower critical solution temperature) could reduce from 42 ^{o}C to 30 ^{o}C. The morphology change of freeze dried samples below and above LCST proves that the phase change of this hydroxypropylcellulose based hydrogel is due to the solubility change of polymer in water. The fine-tuned recipe can give an outstanding solar modulating ability (ΔT_{sol}) of 25.7% and high averaged T_{lum} of 67.4% with LCST of 38 ^{o}C.

Introduction

Hydroxypropylcellulose (HPC) is a water-soluble cellulose derivative, which is usually synthesized by the reaction of propylene oxide on cellulose under alkaline conditions, producing

lateral chains containing a variable number of hydroxypropoxy groups.[1] Numerous new functional materials of hydroxypropylcellulose have being developed over a broad range of applications because of the increasing demand for environmentally friendly and biocompatible requirement.[2] The general properties of HPC include biodegradable, non-toxic and solid polymer.[3] It has a molecular structure of D-anhydroglucopyranose units that are joined together by β-1,4-glucosidic bonds.[4] For each anhydroglucose unit, it has three reactive –OH (hydroxyl) sites and this allow the polymer to form stable structures through hydrogen bonding.[5] It is a very renewable resource that has a number of traditional applications including biological, medical and pharmaceutical fields.[6-12]

Thermochromic materials are the most cost effective smart window materials which can regulate solar transmission automatically without any extra energy input. An ideal thermochromic smart-window material require a large solar modulation (ΔT_{sol}), near room temperature critical temperature (τ_c) and high luminous transmission (T_{lum}).[13] Inorganic materials based vanadium dioxide (VO_2) are common used in smart windows.[14, 15] To attain good thermochromic properties, much efforts such as doping (such as Mg^{2+}/W, rare earth doping such as Tb, La and Eu^{3+}),[16-21] antireflective coating,[22, 23] nanoporus structuring,[24-26] nanoparticle-based composites[27-32] and biomimetic nanostructuring[33, 34] and nanogriding[35] have been investigated. However, the intrinsic physical properties of VO_2 of large luminous absorption at both high and low temperature render it difficult to improve ΔT_{sol} and high T_{lum} simultaneously.[36] In the previous work, temperature-responsive hydrogels and binary solvent colloids PNIPAm films used for smart windows have been reported,[37, 38] and adding co-solvent could change the LCST of PNIPAm hydrogels. However due to the complicated fabrication approach and the difficult in controlling the gelation time and removing the odor, environmental friendly HPC is

experimented as candidates to replace PNIPAm based hydrogel for using in smart windows with lowered τ_c. In this paper, we report a facile way of preparing HPC based thermochromic material and extend its application in smart windows.

Experimental

Materials

The chemicals used in this study were HPC (MW. 100,000, 99% purification, Sigma-Aldrich), NaCl (Sigma-Aldrich), Disperbyk 180 (Sigma-Aldrich) and a multipurpose sealant (Selleys All Clear). Deionized water (18.2 MΩ) was used throughout the experiments. All chemicals were used as received without any further purification.

Preparation of HPC/NaCl solution films

0.05 g HPC powder was mixed in 10 mL deionized water (0.5% w/w) to form HPC solvent by gently stirring for one day to ensure it thoroughly dissolved. 0.05 g NaCl was added to the solution to form HPC/NaCl hybrid solution (0.5% NaCl w/w). The 0.1% and 5% NaCl solutions were prepared as the same method. Samples with 0.35 mm, 0.7 mm and 1.4 mm films were made with various NaCl concentrations and the sealant was applied at the edges to prevent mass exchange with the outside environment.

Characterization

SEM

The surface morphologies of the HPC were determined by a field emission scanning electron microscope (FESEM, JSM-6340F, JEOL) with an operating voltage of 5 kV. Took 0.05 g HPC sample and dissolved it in 10 mL water sufficiently, then took two 1 mL HPC hydrogel samples

and injected them to plastic vales separately. Heated one sample to 70 ^{o}C for 5 minutes and injected the two samples into nitrogen liquid immediately, freeze drying the 2 samples and SEM was tested.

UV-VIS-NIR

The UV-VIS-NIR (Cary 5000, Agilent, USA) spectra were tested using wavelength range 250-2500 nm at 10 nm/s incidence. The spectrophotometer was equipped with a heating and cooling stage (PE120, Linkam, UK). A baseline correction was first conducted within wavelength ranging from 2500 nm to 250 nm before running the sample tests. In our case, the sample was injected into a "glass box" to form sample film. Pose the substrate properly to ensure that the beam is aligned to center of the substrate. All the tests were run at 20 °C and 45 °C respectively and results of transmittance *vs* wavelength were obtained. The calculation of integral luminous transmittance, T_{lum} (380-780 nm), infrared transmittance, T_{IR} (780-2500 nm) and solar transmittance, T_{sol} (250-2500 nm) and $\Delta T_{lum/IR/sol}$ can be found elsewhere.[37]

Differential Scanning Calorimetry (DSC)

DSC test was conducted for pure HPC solution which was prepared from HPC white powder and deionized (DI) water. The sample was weighed at 8.176mg for HPC and 7.983 mg for HPC/NaCl (5%) placing in a hermetic aluminum pan. It was then covered using a hermetic aluminum lid and clamped using a press before loaded into a TA Instruments Q10 DSC. A reference pan (empty) was loaded as well. The sample was heated from 20 ºC to 60 ºC and cooled back to 20 ºC at the rate of 10 ºC per minute. The run was operated under nitrogen atmosphere at 50 mL per min. The heating flow rate of the sample was then recorded against a reference pan.

Results and discussion

As shown in Fig 1a, the visible light transmittance of HPC is dramatically decreased when the temperature heated from 20 ^{o}C to 44 ^{o}C with negligible IR change. This is reflected that the solution changes from transparent at 20 ^{o}C to translucent at 42 ^{o}C (Fig. 1b). It is worth noting that the reduction in transmittance at around 1430 and 1930 nm for both high and low temperature is due to the absorption of water at these two wavelengths.[39] When the temperature increased to 50 ^{o}C, large reduction of transmission of both visible and IR range is observed and the solution turns more opaque. When the temperature increase to 60 ^{o}C and 70 ^{o}C, it turns completely opaque and all the transmission from 250 to 2500nm are blocked. It can be recovered to transparency within 1 min after removing the heater.

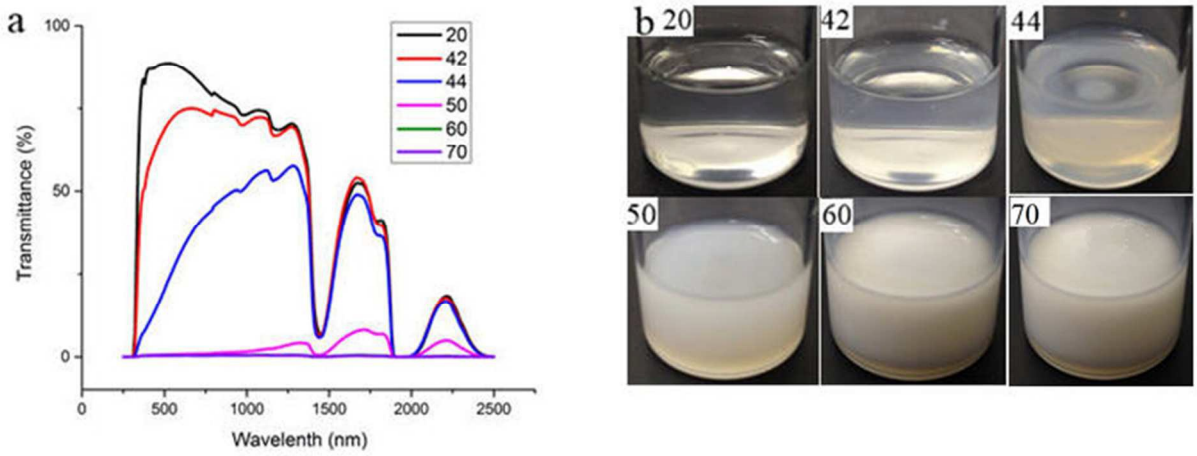

Fig. 1(a) Optical transmittance spectra of the 0.35 mm HPC sample with temperature from 25 ^{o}C to 50 ^{o}C. (b) Pictures of various temperatures of HPC.

The HPC hydrogel at both 20 and 70 ^{o}C were freeze dried and remaining power was examined by SEM. The polymer fibers at room temperature is around 10 μm in diameter with the pores size (occupied by water before freeze drying) larger than 20 μm. At 70 ^{o}C, the remaining

polymer web structure with much diminished size of around 2 μm, accompanying with the largely contracted pore size of less than 10 μm. It is well known that the pure HPC is more soluble in water at the temperatures below LCST (44 °C) than it is at the temperatures above the LCST.[40-42] The water driven out from the HPC fiber above LCST causes the shrinkage; the much smaller pores and closed packed polymeric web structure act as a scattering center to block the visible light and result in opaque status above LCST (Fig. 1b).

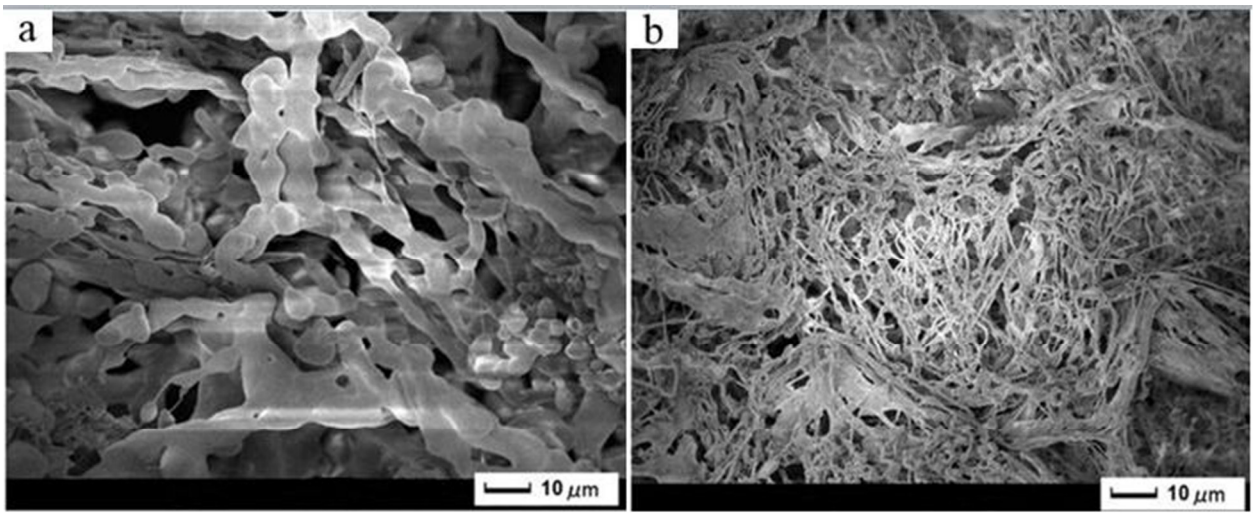

Fig. 2 SEM image of freeze dried HPC hydrogel at (a) 20 ^{o}C and (b) 70 ^{o}C.

The transmittance at a fixed wavelength of 580 nm in the temperature range of 20 to 60 °C was recorded in a heating and cooling cycle and plotted as %*T versus T*/°C hysteresis loops (Fig. 3a). The LCST of pure HPC is 44 °C, when 0.5% NaCl was added, the τ_c was decreased to 38 °C. 1% NaCl will induce the τ_c of HPC slightly decreased to 35 °C. The inset shows that the NaCl can largely reduce τ_c at the concentration as small as 0.5%, while τ_c of HPC could only marginally reduce to 30 °C with the addition of NaCl up to 5%.

As shown in Fig 3b, DSC suggests that LCST of pure HPC is 46 ^{o}C, with dramatically reduced LCST to 38 ^{o}C when adding 0.5% NaCl. When the concentration of NaCl increases to 5%, the τ_c of HPC could reduce to 31 ^{o}C. In pure HPC, at low temperatures more hydrogen bonds exist between water and the HPC polymer fibers, as the temperature increases, these hydrogen bonds are gradually broken, indicating a continuous phase separation. By adding NaCl, the hydrogen bonding between HPC and water weakens, facilitating the formation of finer polymeric web structure, which acts as a scattering center to block the visible light, resulting in opaque status above LCST.[43]

The solar light transmittance (250-2500 nm) profiles at 20 °C and 45 °C are shown in Fig. 3c with fixed thickness of 0.35 mm for all samples. For pure HPC film, it has the highest solar transmittance for both temperatures. $T_{lum(20\ °C)}$ for all the samples are larger than 80% remains constant (Table 1). Both $T_{lum(45\ °C)}$ and $T_{sol(45\ °C)}$ decrease with increasing NaCl concentration from 0.5% to 5%, which is due to the reduced LCST (Fig. 3a). As can be seen from Fig. 3d, the ΔT_{sol}, $\Delta T_{IR,}$ ΔT_{lum} were all increased with increasing NaCl concentration. For HPC/NaCl (0.5%) sample, the ΔT_{sol} is 25.7% with high averaged T_{lum} at 67.4 % (Table 1), which indicates it is a suitable candidate for smart window application.

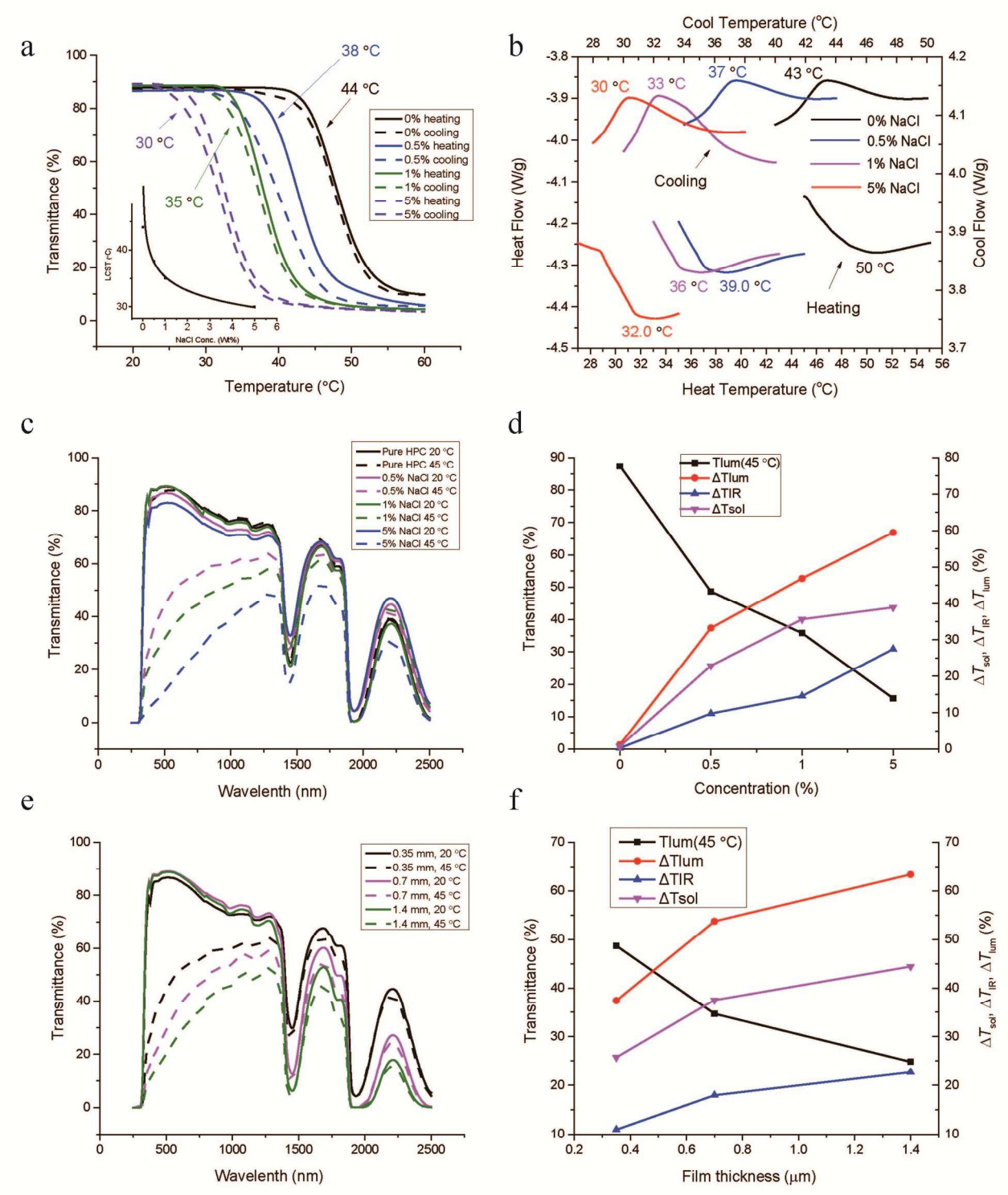

Fig. 3 (a). Hysteresis loop for the temperature-dependent transmittance of the HPC/NaCl (0-5%) samples with 0.7 mm thickness at a wavelength 580 nm and the curve of LCST *vs* NaCl

concentration (Wt%). (b) DSC spectra of pure HPC and HPC/NaCl samples. (black: 0% NaCl; blue: 0.5% NaCl; purple: 1% NaCl; red: 5% NaCl) (c) Optical transmittance spectra of 0.35 mm HPC/NaCl samples at both 20 and 45 ^{o}C. (d) Concentration effects on ΔT_{sol}, ΔT_{lum}, ΔT_{IR} and T_{lum} at 45 ^{o}C. (e) Optical transmittance spectra of 0.35, 0.7 and 1.4 mm thickness of HPC/NaCl (0.5%) samples. (f) Thickness influence on ΔT_{sol}, ΔT_{lum}, ΔT_{IR} and T_{lum} (45 ^{o}C) of HPC/NaCl (0.5%) samples.

Table 1. Comparison of optical properties between different NaCl concentrations with 0.35 mm HPC films.

Con. (%)	$T_{lum(20\ °C)}$	$T_{lum(45\ °C)}$	ΔT_{lum}	**Ave. T_{lum}**	$T_{sol(20\ °C)}$	$T_{sol(45\ °C)}$	ΔT_{IR}	**ΔT_{sol}**	τ_c (°C)
0	88.4	87.5	1.3	**88.1**	79.2	78.4	0.3	**0.8**	**44**
0.5	86.1	48.7	37.4	**67.4**	76.5	50.8	11.0	**25.7**	**38**
1	88.5	35.8	52.7	**60.0**	78.2	38.1	16.4	**40.1**	**35**
5	82.5	15.6	66.9	**51.2**	66.9	23.3	30.9	**43.6**	**30**

For the HPC/NaCl (0.5%) films of 0.35 to 1.4 mm thickness, transparency drops significantly when the temperature rises from 20 ^{o}C to 45 ^{o}C (Fig. 3e), which indicates that there is phase change below 45 ^{o}C for HPC. The water absorption intensity at both 1930 and 1430 nm increased when the thickness increased from 0.35 to 1.4 mm due to higher volume of water. Similar to NaCl concentration effects, $T_{lum(20\ °C)}$ remained nearly unchanged for all three thickness, whereas $T_{lum(45\ °C)}$ underwent a gradually reduction from ~50% (0.35 mm) to 25% (1.4 mm). Although the 1.4 mm thick HPC/NaCl (0.5%) solution showed an much higher ΔT_{sol} value of 45%, its low $T_{lum(45\ °C)}$ of less than 25% is not favored for an ideal smart window. The

averaged $T_{lum(45\ °C)}$ decreases with increasing thickness, while ΔT_{sol}, ΔT_{lum}, ΔT_{IR} increase with increasing thickness (Fig. 3f).

Importantly, the good performance was maintained in the durability test. The UV lighting set was employed in the durability test experiment. Pure HPC/NaCl (0.5%) sample was exposed under the UV light up to 10 days and the T_{lum} at both high and low temperatures and ΔT_{sol} remain constant, indicating that the performance stability should be reliable under the exposure of UV in the normal outdoor conditions.

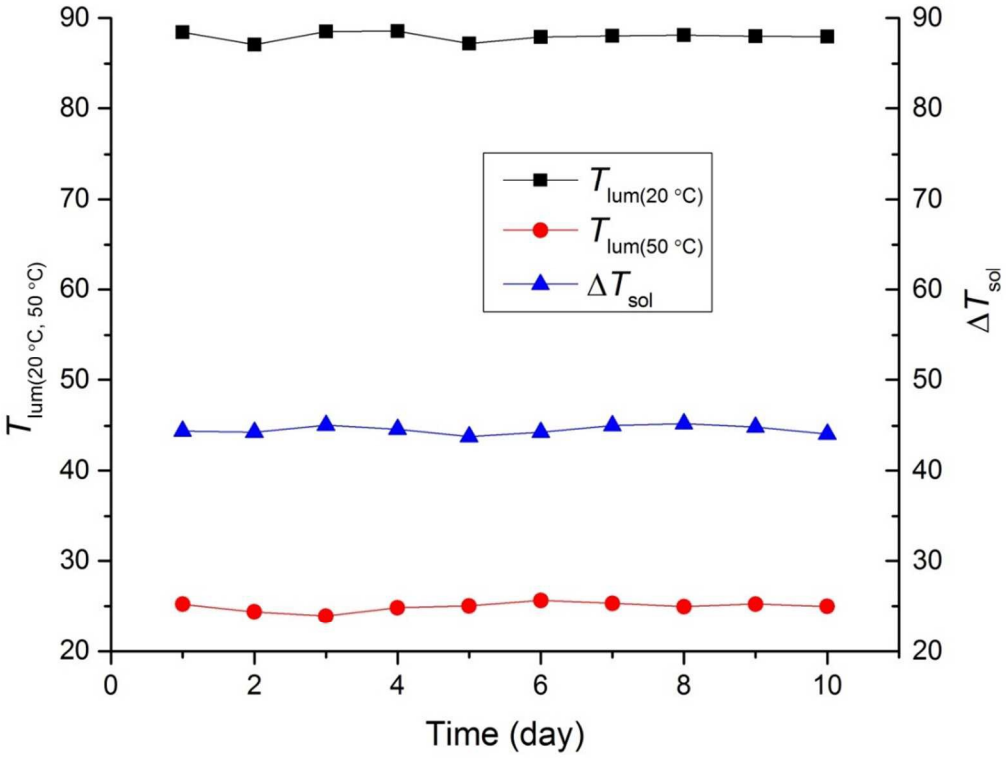

Fig. 4 Durability test of HPC/NaCl (0.5%) with thickness of 0.35 mm between 20 and 50 ^{o}C.

Conclusion

Temperature-responsive HPC and HPC/NaCl solutions were investigated as potential thermochromic materials for smart window applications. The hydrogels can be totally transparent at room temperature, with a high T_{lum} of 86.1%, and translucent at 45 ^{o}C, with an acceptable T_{lum} of 48.7%. Meanwhile it can provide both high modulation in the visible range and moderate modulation ability in the IR range, which lead overall to an enhanced $\Delta T_{sol(20–45\ °C)}$ of 25.7%. The HPC/NaCl samples showed a good combination of high T_{lum}, dramatically improved ΔT_{sol} and lowered transition temperature with good durability and reversibility.

Acknowledgments:

This research is supported by Singapore Minster of Education (MOE) Academic Research Fund Tier 1 RG101/13 and NRF2015NRF-POC002-019.

Notes and references:

1. S. Fortin and G. Charlet, *Macromolecules*, 1989, **22**, 2286-2292.
2. D. Klemm, B. Heublein, H.-P. Fink and A. Bohn, *Angew. Chem. Int. Ed.*, 2005, **44**, 3358-3393.
3. Y. Nishio, *Cellulosic polymers, blends and composites*, 1994, 5.
4. J.-L. Wertz, J. P. Mercier and O. Bédué, *Cellulose science and technology*, CRC Press, 2010.
5. F. Malara, A. Cannavale, S. Carallo and G. Gigli, *ACS Appl. Mater. Inter.*, 2014, **6**, 9290-9297.
6. D. Richardson, E. J. Lindley, C. Bartlett and E. J. Will, *Am. J. Kidney Dis.*, 2003, **42**, 551-560.
7. R. a. Rodríguez, C. Alvarez-Lorenzo and A. Concheiro, *J. Control. Release*, 2003, **86**, 253-265.
8. J. Siepmann, K. Podual, M. Sriwongjanya, N. Peppas and R. Bodmeier, *J. Pharm. Sci.*, 1999, **88**, 65-72.
9. Y. Suzuki and Y. Makino, *J. Control. Release*, 1999, **62**, 101-107.
10. M. F. Francis, M. Piredda and F. M. Winnik, *J. Control. Release*, 2003, **93**, 59-68.
11. C. R. Park and D. L. Munday, *Int. J. Pharm.*, 2002, **237**, 215-226.
12. J. Siepmann and N. Peppas, *Adv. Drug Del. Rev.*, 2012, **64**, 163-174.
13. S.-Y. Li, G. A. Niklasson and C. G. Granqvist, *J. Appl. Phys.*, 2010, **108**, 063525.
14. N. Wang, S. Magdassi, D. Mandler and Y. Long, *Thin Solid Films*, 2013, **534**, 594-598.
15. S. Wang, M. Liu, L. Kong, Y. Long, X. Jiang and A. Yu, *Prog. Mater Sci.*, 2016, **81**, 1-54.
16. N. Wang, M. Duchamp, R. E. Dunin-Borkowski, S. Liu, X. Zeng, X. Cao and Y. Long, *Langmuir*, 2016, **32**, 759-764.
17. N. Wang, S. Y. Liu, X. T. Zeng, S. Magdassi and Y. Long, *J. Mater. Chem. C*, 2015, **3**, 6771-6777.
18. X. Cao, N. Wang, S. Magdassi, D. Mandler and Y. Long, *Sci. Adv. Mater.*, 2014, **6**, 558-561.
19. N. Mlyuka, G. Niklasson and C.-G. Granqvist, *Appl. Phys. Lett.*, 2009, **95**, 171909.

20. N. Wang, N. Tan Chew Shun, M. Duchamp, R. E. Dunin-Borkowski, Z. Li and Y. Long, *Rsc Adv.*, 2016, **6**, 48455-48461.
21. N. Wang, M. Duchamp, C. Xue, R. E. Dunin-Borkowski, G. Liu and Y. Long, *Adv. Mater. Interfaces*, 2016, DOI: 10.1002/admi.201600164.
22. C. Liu, N. Wang and Y. Long, *Appl. Surf. Sci.*, 2013, **283**, 222-226.
23. Z. Chen, Y. Gao, L. Kang, J. Du, Z. Zhang, H. Luo, H. Miao and G. Tan, *Sol. Energy Mater. Sol. Cells*, 2011, **95**, 2677-2684.
24. X. Cao, N. Wang, J. Y. Law, S. C. J. Loo, S. Magdassi and Y. Long, *Langmuir*, 2014, **30**, 1710-1715.
25. L. Kang, Y. Gao, H. Luo, Z. Chen, J. Du and Z. Zhang, *ACS Appl. Mater. Inter.*, 2011, **3**, 135-138.
26. N. Wang, Y. Z. Huang, S. Magdassi, D. Mandler, H. Liu and Y. Long, *Rsc Adv.*, 2013, **3**, 7124-7128.
27. P. Liu, L. A. Liu, K. L. Jiang and S. S. Fan, *Small*, 2011, **7**, 732-736.
28. X. Chen, L. Liu, K. Liu, Q. Miao and Y. Fang, 2014, **2**, 2718-2727.
29. Z. Chen, Y. Gao, L. Kang, C. Cao, S. Chen and H. Luo, *Journal of Materials Chemistry A*, 2014, **2**, 2718-2727.
30. Y. F. Gao, S. B. Wang, L. T. Kang, Z. Chen, J. Du, X. L. Liu, H. J. Luo and M. Kanehira, *Energy Environ. Sci.*, 2012, **5**, 8234-8237.
31. X. Cao, M. N. Thet, Y. Zhang, S. C. J. Loo, S. Magdassi, Q. Yan and Y. Long, *Rsc Adv.*, 2015, **5**, 25669-25675.
32. C. Liu, X. Cao, A. Kamyshny, J. Y. Law, S. Magdassi and Y. Long, *Journal of Colloid and Interface Science*, 2014, **427**, 49-53.
33. X. Qian, N. Wang, Y. Li, J. Zhang, Z. Xu and Y. Long, *Langmuir*, 2014, **30**, 10766-10771.
34. A. Taylor, I. Parkin, N. Noor, C. Tummeltshammer, M. S. Brown and I. Papakonstantinou, *Opt. Express*, 2013, **21**, A750-A764.
35. C. Liu, I. Balin, S. Magdassi, I. Abdulhalim and Y. Long, *Optics Express*, 2015, **23**, A124-A132.
36. Y. Zhou, Y. Cai, X. Hu and Y. Long, *J. Mater. Chem. A*, 2015, **3**, 1121-1126.
37. Y. Zhou, Y. Cai, X. Hu and Y. Long, *J. Mater. Chem. A*, 2014, **2**, 13550-13555.
38. M. Wang, Y. Gao, C. Cao, K. Chen, Y. Wen, D. Fang, L. Li and X. Guo, *Industrial & Engineering Chemistry Research*, 2014, **53**, 18462-18472.
39. G. Wyszecki and W. Stiles, Wiley-Interscience, New York.
40. G. Karlstroem, A. Carlsson and B. Lindman, *J. Phys. Chem.*, 1990, **94**, 5005-5015.
41. T. Ahlnäs, G. Karlström and B. Lindman, *J. Phys. Chem.*, 1987, **91**, 4030-4036.
42. G. Karlström, *J. Phys. Chem.*, 1985, **89**, 4962-4964.
43. X. Xia, S. Tang, X. Lu and Z. Hu, *Macromolecules*, 2003, **36**, 3695-3698.

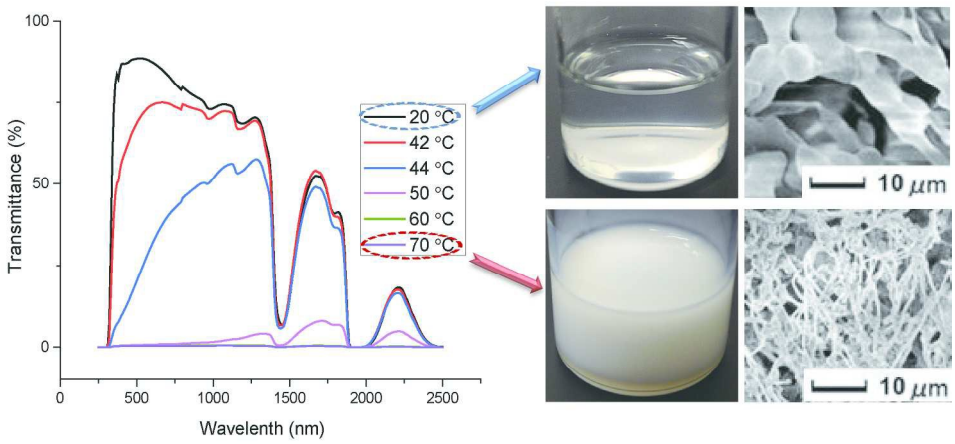

203x114mm (300 x 300 DPI)